Icarus 373 (2022) 114799

Contents lists available at ScienceDirect

Icarus

journal homepage: www.elsevier.com/locate/icarus

Crystalline ices – Densities and comparisons for planetary and interstellar applications

Yukiko Y. Yarnall [a,b], Reggie L. Hudson [a,*]

[a] Astrochemistry Laboratory, NASA Goddard Space Flight Center, Greenbelt, MD 20771, USA
[b] Universities Space Research Association, Greenbelt, MD 20771, USA

ARTICLE INFO

Keywords:
Ices
IR spectroscopy
TNOs
Titan
Organic chemistry

ABSTRACT

Results are presented from recent density measurements on twenty-nine crystalline ices at temperatures applicable to the outer Solar System and the interstellar medium. For each ice we report both a density and a refractive index at 670 nm, quantities needed to calculate infrared band strengths, complex indices of refraction, and, ultimately, molecular abundances. Comparisons are made between densities obtained from micrometer-size crystalline ice samples prepared by vapor-phase deposition and the larger crystals (mm scale) used in diffraction work, and often made by the slow cooling of a liquid or a vapor in a sealed capillary tube. A strong positive correlation is found between the two sets of crystalline-ice densities.

Considerable low-temperature laboratory work on extraterrestrial ices has focused on infrared (IR) spectra and other properties of amorphous molecular solids with one or more components, sometimes to the neglect of crystalline solids. This is unfortunate as crystalline compounds can be found in multiple Solar System environments. For example, crystalline H_2O-ice is fairly common within our Solar System, Titan's temperatures certainly are high enough for crystalline nitriles to form, and the temperatures on Pluto suggest the presence of crystalline phases of both methane (CH_4) and nitrogen (N_2). See, among many examples, papers by Jewitt and Luu (2004), Hansen and McCord (2004), Maynard-Casey et al. (2020), and Cable et al. (2021). It is the purpose of the present brief paper (i) to present new data on crystalline solids from measurements under vacuum at roughly 10 to 150 K and (ii) to compare crystalline-ice densities obtained with different methods usually under different sets of conditions by two different scientific communities.

Infrared spectra of crystalline solids at astrochemically relevant temperatures have been published going back to at least the late 1940s (Hoffman and Hornig, 1949), but such work has tended to emphasize the positions (i.e., wavenumbers, wavelengths) of absorption bands to the exclusion of spectral intensities. The integrated absorbance of an IR band of an icy solid is related to the column density (N) of absorbing ice molecules by

$$2.303 \int_{band} (Absorbance)\, d\tilde{\nu} = (A')\, N \qquad (1)$$

where A' is the band strength (IR intensity) of the spectral feature of interest and 2.303 converts absorbance (base-10 logarithmic scale) to optical depth (base-e logarithmic scale). Column density can be written as $N = \rho_N\, h$, where h is the IR path length through the sample and number density ρ_N is calculated from Avogadro's constant (N_A) and the molar mass (M) of the sample's molecules as $\rho_N = (N_A\ /\ M)\ \rho$. Substituting these expressions into eq. (1) gives

$$2.303 \int_{band} (Absorbance)\, d\tilde{\nu} = \left(A' \frac{N_A}{M}\, \rho \right) h \qquad (2)$$

Eq. (2) is the relevant relation for determining an IR band strength (A') by integrating over an IR feature of interest (Hollenberg and Dows, 1961). However, eq. (2) shows that determinations of A' of an ice require a knowledge of both the ice's density (ρ) and the path length (h) of an IR beam through the sample. In our own work, interference fringes combined with a reference refractive index, n, of the ice give the ice's thickness (h), which in our measurements is also the IR path length through the sample (e.g., Hudson et al., 2014a; Hudson et al., 2014b; Hudson et al., 2017; Hudson et al., 2021). The point we wish to emphasize is that in eq. (2) a crystalline ice's density ρ is needed to calculate an IR band strength A', and that band strengths are needed to determine molecular abundances from laboratory, spacecraft, and telescopic data.

The usual approach to working with eq. (2) for crystalline ices made by vapor-phase deposition has been to adopt a density from the x-ray

* Corresponding author at: Astrochemistry Laboratory (Code 691), NASA Goddard Space Flight Center, Greenbelt, MD 20771, USA.
E-mail address: reggie.hudson@nasa.gov (R.L. Hudson).

https://doi.org/10.1016/j.icarus.2021.114799
Received 13 October 2021; Received in revised form 11 November 2021; Accepted 11 November 2021
Available online 14 November 2021
0019-1035/Published by Elsevier Inc.

diffraction literature, where crystals typically are larger and not always grown under vacuum. The underlying assumption is that the densities of crystals grown by the two methods are similar, and so densities from crystallographic studies can be used for IR samples made by a different procedure, such as vapor-phase deposition. We are not aware, however, that this assumption, going back about 60 years or more (e.g., Wieder and Dows, 1962), has been tested. Therefore, here we report new density measurements for over two dozen crystalline ices prepared under vacuum and we compare our results to densities from the diffraction literature. Along with our density measurements, we also have determined n values at 670 nm for these same ices, quantities needed for accurate calculations of IR optical constants (i.e., complex indices of refraction), which in turn are used for modeling of icy surfaces in our solar system.

The details of our laboratory methods and equipment are described in recent papers from our group, so only a summary is needed here. Briefly, crystalline ices were grown by background deposition of a vapor or gas onto the pre-cooled gold-plated substrate of a quartz-crystal microbalance (QCM) within an ultra-high vacuum (UHV) chamber ($\sim 10^{-10}$ Torr). We simultaneously recorded changes in the intensities of two laser beams ($\lambda = 670$ nm) reflected from the ice and substrate, the periods of the lasers giving n, the ice's refractive index (Tempelmeyer and Mills, 1968). Ice thicknesses were on the order of 1 μm, with ices being made with deposition rates that gave an increase in the resulting ice's thickness of 1 to 3 μm hr^{-1}. Typical uncertainties expressed as standard errors in n and ρ are at worse ±0.01 and ± 0.01 g cm^{-3}, respectively, and more typically ±0.005 and ± 0.005 g cm^{-3}. Each n and ρ we report is an average of at least three measurements. See recent papers from our group (e.g., Hudson et al., 2017; Hudson et al., 2020) or elsewhere (e.g., Satorre et al., 2008) for additional experimental details and background information.

To compare densities measured in our vacuum system with those from diffraction work, we selected twenty-nine molecular ices from the crystallographic literature. The ices were chosen partly for their astronomical relevance, but also to cover a wide variety of molecular classes. Specifically, the crystalline ices selected included those involving polar and non-polar molecules, covalent and ionic bonding, and aliphatic and aromatic organics. In a few cases, the crystallographic densities had to be interpolated between published values, taken from figures after digitizing, or recalculated from unit-cell dimensions.

Fig. 1 compares the densities we measured to those from the crystallographic literature. Table 1 lists the densities plotted, names and formulas of compounds, temperatures, and our measured refractive indices. In Table 1, crystalline hydrocarbon ices are listed first, followed by C-, H-, and O-containing organic compounds, and then C-, H-, and N-containing organic compounds. The last ten entries are for inorganics, seven without sulfur and then three with sulfur. References are given for all twenty-nine entries taken from the literature. That our ices were indeed crystalline at the temperatures listed was confirmed by recording their IR spectra and observing the sharpening and so forth that indicate crystallinity, compared to that found in the IR spectra of amorphous solids.

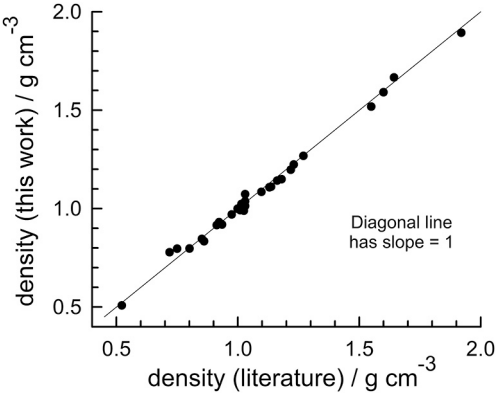

Fig. 1. Comparison of densities of twenty-nine crystalline ices made by vapor-phase deposition (this work) and ice densities from diffraction studies (literature). See Table 1 for the densities plotted.

Table 1
Densities and refractive indices of crystalline ices.

		This Work			Literature	
No.	Formula, Name	T[a]	n[a]	ρ[a]	ρ[a]	T[a]
1	CH_4, methane	30	1.333	0.508	0.522[b]	30
2	C_2H_6, ethane	60	1.496	0.778	0.719[c]	85
3	C_3H_8, propane	65	1.484	0.797	0.801[d]	65
4	C_2H_4, ethylene	60	1.513	0.796	0.750[e]	85
5	c-C_3H_6, cyclopropane	65	1.512	0.916	0.913[f]	100
6	C_6H_6, benzene	100	1.620	1.085	1.097[g]	270
7	$(CH_3)_2CO$, acetone	125	1.453	0.999	0.999[h]	110
8	CH_3OH, methanol	120	1.444	1.023	1.015[i]	160
9	C_2H_5OH, ethanol	120	1.474	0.989	1.025[j]	87
10	CH_3COOH, acetic acid	150	1.485	1.268	1.27[k]	269
11	CH_3COOCH_3, methyl acetate	115	1.484	1.197	1.218[l]	145
12	$HC(O)CH_3$, acetaldehyde	100	1.486	1.111	1.137[m]	5
13	$(CH_3)_2O$, dimethyl ether	75	1.441	0.970	0.975[n]	93
14	c-OC_2H_4, ethylene oxide	100	1.458	1.142	1.162[o]	100
15	CH_3NH_2, methylamine	100	1.460	0.861	0.852[p]	123
16	$C_2H_5NH_2$, ethylamine	100	1.508	0.924	0.935[q]	150
17	CH_3CN, acetonitrile	130	1.495	1.073	1.030[r]	201
18	C_2H_5CN, propionitrile	110	1.467	0.992	1.010[s]	100
19	C_5H_5N, pyridine	120	1.588	1.149	1.180[t]	153
20	H_2O, water	150	1.329	0.931	0.935[u]	143
21	NH_3, ammonia	95	1.438	0.834	0.861[v]	77
22	HCN, hydrogen cyanide	120	1.428	1.037	1.030[w]	153
23	CO_2, carbon dioxide	70	1.398	1.666	1.643[x, y]	150
24	N_2O, nitrous oxide	70	1.424	1.591	1.60[y, z]	77
25	N_2, nitrogen	19	1.252	1.013	1.03[b]	19
26	NH_4CN, ammonium cyanide	125	1.550	1.108	1.13[aa]	194
27	H_2S, hydrogen sulfide	80	1.633	1.224	1.230[bb]	80
28	OCS, carbonyl sulfide	50	1.574	1.518	1.549[cc]	90
29	SO_2, sulfur dioxide	85	1.480	1.893	1.92[dd]	143

[a] Temperatures are in kelvins, n is at 670 nm, and densities are in g cm^{-3}.
[b] Maynard-Casely et al. (2020).
[c] Van Nes and Vos (1978).
[d] Boese et al. (1999).
[e] van Nes (1978).
[f] Nijveldt and Vos (1988).
[g] Cox and Smith (1954).
[h] Allan et al. (1999).
[i] Torrie et al. (2002).
[j] Jönsson (1976).
[k] Jones and Templeton (1958).
[l] Barrow et al. (1981).
[m] Ibberson et al. (2000).
[n] Vojinovic et al. (2004).
[o] Grabowsky et al. (2008).
[p] Atoji and Lipscomb (1953).
[q] Maloney et al. (2014).
[r] Enjalbert and Galy (2002).
[s] Brand et al. (2020).
[t] Mootz and Wussow (1981).
[u] Blackman and Lisgarten (1957).
[v] Olovsson and Templeton (1959).
[w] Dulmage and Lipscomb (1951).
[x] Simon and Peters (1980).
[y] de Smedt and Keesom (1924).
[z] Hamilton and Petrie (1961).
[aa] Lely and Bijvoet (1944).
[bb] Calculated from Cockcroft and Fitch (1990).
[cc] Overell et al. (1982).
[dd] Post et al. (1952).

It is obvious in Fig. 1 that although some points deviate from the diagonal line, the overall trend indicates good agreement between the

two sets of data. Note especially that the diagonal line shown is simply a line with a slope of 1 and not a least-squares fit of the data. The closeness of the points in Fig. 1 to the diagonal line suggests that our ices possessed a high degree of crystallinity. These measurements address the lack of published comparisons, already mentioned, between (a) densities obtained from crystals made by vapor-phase deposition as used in many astrochemical laboratories and (b) densities reported by crystallographers, often from samples grown by slow cooling of a liquid or vapor in a sealed capillary tube, and sometimes with densities found by floatation measurements. Moreover, Fig. 1 also provides a check on and builds confidence in the QCM method for laboratory studies of astronomical ice analogs.

Our Fig. 1 and Table 1 are convenient sources of densities, and not just for the temperatures listed. Microbalance measurements to obtain ice densities are less common than interferometric measurements to determine ice refractive indices. However, by combining our n and ρ values in Table 1 with the Lorentz-Lorenz relation, eq. (3) below, one can estimate the density of a crystalline ice using only a refractive index measurement at the temperature of interest, the molar refraction R_M being roughly constant with temperature.

$$R_M = \left(\frac{M}{\rho}\right)\left(\frac{n^2-1}{n^2+2}\right) \tag{3}$$

The results of our Table 1 and Fig. 1 show that the density of a crystalline ice grown in a capillary by freezing a liquid or condensing a vapor is similar to that of an ice formed by vapor-phase condensation in a vacuum chamber. Therefore, if the density of an ice condensed from a vapor under vacuum is needed then it is indeed safe to adopt a value from diffraction work, a long-standing, but unchecked, practice in the spectroscopic community (e.g., Yamada and Person, 1964). Conversely, if an ice density is not available from a diffraction study then one can be confident that a density measured with a QCM will be close to the desired quantity. As an example from our own work, we have not yet located a density of solid allene, a Titan molecule (Lombardo et al., 2019), from a diffraction study, but we believe that a reasonable value can be found with the methods used here. The same applies to thiols, compounds with such offensive odors and high toxicity that preparing a mm-sized crystal for diffraction work would be unattractive to many. As another example, diazomethane ($H_2C{=}N{=}N$) is readily formed by either the photolysis or radiolysis of solid mixtures of N_2 and CH_4, and is thought to be present on cold outer Solar System objects such as Pluto (e.g., Bohn et al., 1994; Moore and Hudson, 2003). However, diazomethane's explosive instability and high toxicity can discourage measurements on the bulk crystalline solid. The methods outlined here, vapor-phase deposition with small quantities under vacuum, should safely yield n and ρ values. Finally, the close agreement between the densities of our micrometer-thick samples and the densities of the larger crystals used for diffraction work suggests minimal differences due to scaling.

This paper has focused on comparing density values from two different scientific communities and testing the assumption that the values are similar. However, the results summarized in Table 1 and Fig. 1 have other uses, such as assisting with the measurement of ice thicknesses and band strengths that, in turn, aid in the determination of column densities in laboratory and extraterrestrial ices. Our data, along with IR intensities, also can serve as benchmarks with which to compare the results of ab initio, or other, computations of properties of crystalline molecular solids. We plan to continue to generate and improve on such data in the future.

To summarize, we have measured the densities of over two dozen crystalline compounds and compared the results to those from diffraction studies, finding good agreement. Although the vapor-deposition method for density determinations does not provide the structural details of a diffraction study, it can be advantageous in certain cases, such as when a crystallization is difficult, expensive, or even dangerous. Future density comparisons could include CS_2 for cometary studies, O_3 for icy satellites, and CO for trans-Neptunian objects, but given the trend in Fig. 1 we will be surprised if the density of any of these three compounds differs substantially from literature diffraction results.

Declaration of Competing Interest

None.

Acknowledgements

We acknowledge the support of NASA's Planetary Science Division Internal Scientist Funding Program through the Fundamental Laboratory Research (FLaRe) work package at the NASA Goddard Space Flight Center. We also recognize the invaluable laboratory assistance of Perry Gerakines (NASA), Robert Ferrante (US Naval Academy), and Mark Loeffler (University of Northern Arizona).

References

Allan, D.R., Clark, S.J., Ibberson, R.M., Parsons, S., Pulham, C.R., Sawyer, L., 1999. The influence of pressure and temperature on the crystal structure of acetone. Chem. Commun. 751–752.
Atoji, M., Lipscomb, W.N., 1953. On the crystal structures of methylamines. Acta Cryst 6, 770–774.
Barrow, M.J., Cradock, S., Ebsworth, E.A.V., Rankin, D.W.H., 1981. Crystal structures of silyl acetate at 150 K and methyl acetate at 145 K, and the molecular structure of silyl acetate in the gas phase. JCS Dalton 1988–1993.
Blackman, M., Lisgarten, N.D., 1957. The cubic and other structural forms of ice at low temperature and pressure. Proc. Roy. Soc. A. 239, 93–107.
Boese, R., Weiss, H., Bläser, D., 1999. The melting point alternation in the short-chain n-alkanes: single-crystal X-ray analyses of propane at 30 K and of n-butane to n-nonane at 90 K. Angew. Chem. Int. Ed. 38, 988–992.
Bohn, R.B., Sandford, S.A., Allamandola, L.J., Cruikshank, D.P., 1994. Infrared spectroscopy of Triton and Pluto ice analogs: the case for saturated hydrocarabons. Icarus 111, 151–173.
Brand, H.E.A., Gu, Q., Kimpton, J.A., Auchettl Ennis, C., 2020. Crystal structure of propionitrile (CH_3CH_2CN) determined using synchrotron powder X-ray diffraction. J. Synchroton Rad. 27, 212–216.
Cable, M.L., Runčevski, T., Maynard-Casely, H.E., Vu, T.H., Hodyss, R., 2021. Titan in a test tube: organic co-crystals and implications for titan mineralogy. Acc. Chem. Res. 54, 3050–3059.
Cockcroft, J.K., Fitch, A.N., 1990. The solid phases of deuterium sulphide by powder neutron diffraction. Zeit. Für Kristal. 193, 1–19.
Cox, E.G., Smith, J.A.S., 1954. Crystal structure of benzene at −3 °C. Nature 173, 75.
Dulmage, W.J., Lipscomb, W.N., 1951. The crystal structures of hydrogen cyanide. HCN. Acta. Cryst. 4, 330–334.
Enjalbert, R., Galy, J., 2002. CH_3CN: X-ray structural investigation of a unique single crystal. $\beta \rightarrow \alpha$ phase transition and crystal structure. Acta Cryst B58, 1005–1010.
Grabowsky, S., Weber, M., Buschmann, J., Luger, P., 2008. Experimental electron density study of ethylene oxide at 100 K. Acta Cryst B64, 397–400.
Hamilton, W.C., Petrie, M., 1961. Confirmation of disorder in solid nitrous oxide by neutron diffraction. J. Phys. Chem. 65, 1453–1454.
Hansen, G.B., McCord, T.B., 2004. Amorphous and crystalline ice on the Galilean satellites: a balance between thermal and radiolytic processes. J. Geophys. Res. 109, 1.
Hoffman, R.E., Hornig, D.F., 1949. The infra-red spectrum of solid hydrogen cyanide. J. Chem. Phys. 17, 1163.
Hollenberg, J.L., Dows, D.A., 1961. Measurement of absolute infrared absorption intensities in crystals. J. Chem. Phys. 34, 1061–1063.
Hudson, R.L., Ferrante, R.F., Moore, M.H., 2014a. Infrared spectra and optical constants of astronomical ices: I. Amorphous and crystalline acetylene. Icarus 228, 276–287.
Hudson, R.L., Gerakines, P.A., Moore, M.H., 2014b. Infrared spectra and optical constants of astronomical ices: II. Ethane and ethylene. Icarus 243, 148–147.
Hudson, R.L., Loeffler, M.J., Gerakines, P.A., 2017. Infrared spectra and band strengths of amorphous and crystalline N_2O. J. Chem. Phys. 146, 0243304.
Hudson, R.L., Loeffler, M.J., Ferrante, R.F., Gerakines, P.A., Coleman, F.M., 2020. Testing densities and refractive indices of extraterrestrial ice components using molecular structures - organic compounds and molar refractions. Astrophys. J. 891, 1.
Hudson, R.L., Yarnall, Y.Y., Gerakines, P.A., Coones, R.T., 2021. Infrared spectra and optical constants of astronomical ices: III. propane, propylene, and propyne. Icarus 354, 114033.
Ibberson, R.M., Yamamuro, O., Matsuo, T., 2000. Crystal structure and phase behavior of acetaldehyde-d_4: a study by high-resolution neutron powder diffraction and calorimetry. J. Mol. Struct. 520, 265–272.
Jewitt, D.C., Luu, J., 2004. Crystalline water ice on the Kuiper belt object (50000) Quaoar. Nature 432, 731–733.
Jones, E.E., Templeton, D.H., 1958. The crystal structure of acetic acid. Acta Cryst 11, 484–487.

Jönsson, P., 1976. Hydrogen bond studies. CXIII. The crystal structure of ethanol at 87 K. Acta Cryst B32, 232–235.
Lely, J.A., Bijvoet, J.M., 1944. The crystal structure and anisotropic temperature vibration of ammonium cyanide. Rec. Trav. Chim. des Pays-Bas 63, 39–43.
Lombardo, N.A., Nixon, C.A., Greathouse, T.K., Bézard, B., Jolly, A., Vinatier, S., Teanby, N.A., Richter, M.J., Irwin, P.J.G., Coustenis, A., Flasar, F.M., 2019. Detection of propadiene on Titan. Astrophys. J. 881. L33 (6 pp).
Maloney, A.G.P., Wood, P.A., Parsons, S., 2014. Competition between hydrogen bonding and dispersion interactions in the crystal structures of the primary amines. CrystEngComm 16, 3867–3882.
Maynard-Casely, H.E., Hester, J.R., Brand, H.E.A., 2020. *Re*-examining the crystal structure behavior of nitrogen and methane. IUCrJ 7, 844–851.
Moore, M.H., Hudson, R.L., 2003. Infrared study of ion-irradiated N_2-dominated ices relevant to Triton and Pluto: Formation of HCN and HNC. Icarus 161, 486–500.
Mootz, D., Wussow, H.G., 1981. Crystal structures of pyridine and pyridine trihydrate. J. Chem. Phys. 75, 1517–1522.
Nijveldt, D., Vos, A., 1988. Single-crystal X-ray geometries and electron density distributions of cyclopropane, bicyclopropyl and vinylcyclopropane. II. Multipole refinements and dynamic electron density distributions. Acta Cryst B44, 289–296.
Olovsson, I., Templeton, D.H., 1959. X-ray study of solid ammonia. Acta Cryst. 12, 832–836. https://doi.org/10.1107/S0365110X59002420.
Overell, J.S.W., Pawley, G.S., Powell, B.M., 1982. Powder refinement of carbonyl sulphide. Acta Cryst B38, 1121–1123.
Post, B., Schwartz, R.S., Fankuchen, I., 1952. The crystal structure of sulfur dioxide. Acta Cryst 5, 372–374.
Satorre, M.A., Domingo, M., Millán, C., Luna, R., Vilaplana, R., Santonja, C., 2008. Density of CH_4, N_2 and CO_2 ices at different temperatures of deposition. Planet. Space Sci. 56, 1748–1752.
Simon, A., Peters, K., 1980. Single-crystal refinement of the structure of carbon dioxide. Acta Cryst B36, 2750–2751.
de Smedt, J., Keesom, W.H., 1924. The structure of solid nitrous oxide and carbon dioxide. Koninkl. Ned. Akad. Wetenschap. Proc. 27, 839–846.
Tempelmeyer, K.E., Mills, D.W., 1968. Refractive index of carbon dioxide cryodeposit. J. Appl. Phys. 39, 2968–2969.
Torrie, B.H., Binbrek, O.S., Strauss, Swainson, 2002. Phase transitions in solid methanol. J. Solid State Chem. 166, 415–420.
Van Nes, G.J.H., 1978. Single-crystal structures and electron density distributions of ethane, ethylene, and acetylene. PhD Thesis. University of Groningen, the Netherlands.
Van Nes, G.J.H., Vos, A., 1978. Single-crystal structures and electron density distributions of ethane, ethylene, and acetylene. 1. Single-crystal X-ray structure determinations of two modifications of ethane. Acta Cryst B34, 1947–1956.
Vojinovic, K., Losehand, U., Mitzel, N.W., 2004. Dichlorosilane–dimethyl ether aggregation: a new motif in halosilane adduct formation. Dalton Trans. 2578–2581.
Wieder, G.M., Dows, D.A., 1962. Absolute infrared intensities in crystalline C_2H_4 and C_2D_4. J. Chem. Phys. 37, 2990–2995.
Yamada, H., Person, W.B., 1964. Absolute infrared intensities of the fundamental absorption bands in solid CO_2 and N_2O. J. Chem. Phys. 41, 2478–2487.